Journal of Computational Mathematics
Vol.30, No.6, 2012, 657–683.

http://www.global-sci.org/jcm
doi:10.4208/jcm.1208-m4191

GHOST FORCE INFLUENCE OF A QUASICONTINUUM METHOD IN TWO DIMENSION*

Jingrun Chen
South Hall 6705, Mathematics Department, University of California, Santa Barbara, CA93106, USA
ICMSEC, Academy of Mathematics and Systems Science, Chinese Academy of Sciences, Beijing 100190, China
Email: chenjr@lsec.cc.ac.cn
Pingbing Ming
LSEC, ICMSEC, Academy of Mathematics and Systems Science, Chinese Academy of Sciences, Beijing 100190, China
Email: mpb@lsec.cc.ac.cn

Abstract

The error caused by the ghost force is studied for a quasicontinuum method with planar interface in two dimension. For a special case, we derive an analytical expression of the error, which is exploited to prove that the ghost force may lead to a finite size error for the gradient of the solution. The pointwise estimate of the error shows that the error decays algebraically away from the interface, which is much slower than that of the one-dimensional problem, for which the error decays exponentially away from the interface.

Mathematics subject classification: 65N30, 65N12, 65N06, 74G20, 74G15.
Key words: Quasicontinuum method, Ghost force, Interfacial layer.

1. Introduction

Multiscale methods have been developed to simulate mechanical behaviors of solids for several decades [18]. Combination of models at different scales greatly enhances the dimension of problems that computers can deal with. However, problems regarding the consistency, stability and convergence of the multiscale methods may arise from the coupling procedure [3]. Taking the quasicontinuum (QC) method [13, 24] for example, one of the main issues is the so called ghost force problem [22], which is the artificial non-zero force that the atoms experience at the equilibrium state. In the language of numerical analysis, the scheme lacks consistency at the interface between the atomistic region and the continuum region [4]. For the one-dimensional problem, it has been shown in [2, 20] that the ghost force may lead to a finite size error for the gradient of the solution. The error decays exponentially away from the interface.

To understand the influence of the ghost force for high dimensional problems, we study a two-dimensional triangular lattice model with a QC approximation. This QC method couples the Cauchy-Born elasticity model [1] and the atomistic model with a planar interface. Numerical results show that the ghost force may lead to a finite size error for the gradient of the solution as the one-dimensional problem. The error profile exhibits a layer-like structure. Outside the layer, the error decays algebraically.

To further characterize the influence of the ghost force, we introduce a square lattice model with a QC approximation. Compared to the triangular lattice model, this model can be solved

* Received June 5, 2012 / Revised version received July 1, 2012 / Accepted August 7, 2012 / Published online November 16, 2012 /

analytically and the error profile exhibits a clear layer-like structure. Based on the analytical solution, we prove the error committed by the ghost force for the gradient of the solution is $\mathcal{O}(1)$ and the error decays away from the interface to $\mathcal{O}(\varepsilon)$ at distance $\mathcal{O}(\sqrt{\varepsilon}\,)$, where ε is the equilibrium bond length. These are also confirmed by the numerical results. We note that there are some recent efforts devoted to the convergence analysis for ghost force free multiscale coupling methods in high dimension, we refer to [16, 21] and the references therein.

The paper is organized as follows. Numerical results for the triangular lattice model and the square lattice model with QC approximations are presented in § 2 and § 3, respectively. We derive an analytical expression of the solution of the square lattice model with a QC approximation in § 4. The pointwise estimate of the solution is proved in § 5.

2. A QC Method for Triangular Lattice

2.1. Atomistic and continuum models

We consider the triangular lattice $\mathbb{L}$, which can be written as

$$\mathbb{L} = \Big\{ x \in \mathbb{R}^2 \mid x = ma_1 + na_2,\ m, n \in \mathbb{Z} \Big\}$$

with the basis vectors $a_1 = (1, 0), a_2 = (1/2, \sqrt{3}/2)$. Define the unit cell of $\mathbb{L}$ as

$$\Gamma = \Big\{ x \in \mathbb{R}^2 \mid x = c_1 a_1 + c_2 a_2,\ -1/2 \le c_1, c_2 < 1/2 \Big\}.$$

We shall consider lattice system $\varepsilon\mathbb{L}$ inside the domain $\Omega = \Gamma$, and denote $\Omega_\varepsilon = \Omega \cap \varepsilon\mathbb{L}$, where ε is the equilibrium bond length. Assume that the atoms are interacted with the potential function, which is usually a highly nonlinear function, e.g., the Lennard-Jones potential [15]. Denote by $\mathcal{S}_1$ and $\mathcal{S}_2$ the first and the second neighborhood interaction ranges; see Fig. 2.1. In particular, we have

$$\begin{aligned}
&\mathcal{S}_1 = \cup_{i=1}^{6} s_i = \{a_1, a_2, -a_1 + a_2, -a_1, -a_2, a_1 - a_2\},\\
&\mathcal{S}_2 = \cup_{i=7}^{12} s_i = \{a_1 + a_2, -a_1 + 2a_2, -2a_1 + a_2, -a_1 - a_2, a_1 - 2a_2, 2a_1 - a_2\}.
\end{aligned}$$

For $\mu \in \mathbb{Z}^2$, the translation operator T_ε^μ is defined for any lattice function $z : \mathbb{L} \to \mathbb{R}^2$ as

$$(T_\varepsilon^\mu z)(x) = z(x + \varepsilon\mu_1 a_1 + \varepsilon\mu_2 a_2) \quad \text{for } x \in \mathbb{L}.$$

We define the forward and backward discrete gradient operators as

$$D_s^+ = \varepsilon^{-1}(T_\varepsilon^\mu - I) \qquad \text{and} \qquad D_s^- = \varepsilon^{-1}(I - T_\varepsilon^\mu),$$

where $s = \mu_1 a_1 + \mu_2 a_2$ and I is the identity operator. We shall also use the short-hand

$$Dz = (D_1^+ z, D_2^+ z) = (D_{s_1}^+ z, D_{s_2}^+ z).$$

In what follows, we denote $z(x)$ as the deformed positions of the atoms.

Consider an atomic system posed on Ω_ε. The total energy is given by

$$E_{\text{at}}^{\text{tot}} = \frac{1}{2} \sum_{x \in \Omega_\varepsilon} \sum_{s \in \mathcal{S}_1 \cup \mathcal{S}_2} V\left(|D_s^+ z(x)|\right), \tag{2.1}$$

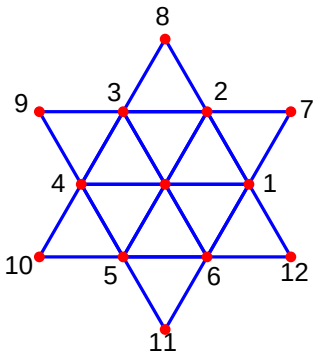

Fig. 2.1. The first and second neighborhood interaction ranges of the triangular lattice; $\mathcal{S}_1 = \{s_1, \cdots, s_6\}$ and $\mathcal{S}_2 = \{s_7, \cdots, s_{12}\}$.

where V is a potential function. In this paper, we only consider the pairwise potential function, and leave the discussion on the more general potential functions in future publication. The atomistic problem is to minimize the total energy subject to certain boundary conditions that will be specified later on.

Next we turn to the Cauchy-Born elasticity model [1, 7–9]. Given a 2 by 2 matrix A, the stored energy density function is given by

$$W_{\mathrm{cb}}(A) = \frac{1}{2\vartheta_0} \sum_{s \in \mathcal{S}_1 \cup \mathcal{S}_2} V(|s \cdot A|),$$

where ϑ_0 is the area of the unit cell and $\vartheta_0 = \sqrt{3}\varepsilon^2/2$. The stored energy function is defined by

$$E_{\mathrm{cb}}^{\mathrm{tot}} = \int_\Omega W_{\mathrm{cb}}(\nabla z(x))\, \mathrm{d}\, x.$$

The continuum problem is to minimize the stored energy function subject to certain boundary conditions. We employ the standard P_1 Lagrange finite element to approximate the Cauchy-Born elasticity model with the lattice $\mathbb{L}$ as the triangulation. The approximate stored energy function is

$$E_{\mathrm{cb},\varepsilon}^{\mathrm{tot}} = \frac{1}{2} \sum_{x \in \Omega_\varepsilon} \sum_{i=1}^{6} \left(V\left(|D_{s_i}^+ z(x)|\right) + V\left(|(D_{s_i}^+ + D_{s_{i+1}}^+) z(x)|\right)\right). \tag{2.2}$$

One can see $E_{\mathrm{cb},\varepsilon}^{\mathrm{tot}}$ reproduces the atomistic energy $E_{\mathrm{at}}^{\mathrm{tot}}$; cf. (2.1), if only the nearest neighborhood interaction is considered.

We study the quasicontinuum method [24]. Let $\varepsilon = 1/(2M)$, and we assume that the interface between the continuum model and the atomistic model is $x_1 = 0$ as shown in Fig. 2.2. The total energy of the QC method is

$$\begin{aligned} E_{\mathrm{qc}}^{\mathrm{tot}} = {} & \frac{1}{2} \sum_{x_1 \le -2\varepsilon} \sum_{i=1}^{6} \left(V\left(|D_{s_i}^+ z(x)|\right) + V\left(|(D_{s_i}^+ + D_{s_{i+1}}^+) z(x)|\right)\right) \\ & + \frac{1}{2} \sum_{x_1 = -\varepsilon} \left\{ \sum_{i=1}^{6} \left(V\left(|D_{s_i}^+ z(x)|\right) + V\left(|(D_{s_i}^+ + D_{s_{i+1}}^+) z(x)|\right)\right) + V(|D_{s_{12}}^+ z(x)|) \right\} \end{aligned}$$

$$+\frac{1}{2}\sum_{x_1=0}\Bigg\{\sum_{s\in\mathcal{S}_1}V\left(|D_s^+z(x)|\right)+\sum_{i=2}^{4}\left(V\left(|D_{s_i}^+z(x)|\right)+V\left(|(D_{s_i}^++D_{s_{i+1}}^+)z(x)|\right)\right)$$
$$+\frac{1}{2}V(|D_{s_7}^+z(x)|)+V(|D_{s_{11}}^+z(x)|)+V(|D_{s_{12}}^+z(x)|)\Bigg\}$$
$$+\frac{1}{2}\sum_{x_1=\varepsilon}\Bigg\{\sum_{s\in\mathcal{S}_1\cup\mathcal{S}_2}V\left(|D_s^+z(x)|\right)-\frac{1}{2}V(|D_{s_9}^+z(x)|)\Bigg\}+\frac{1}{2}\sum_{x_1\geq 2\varepsilon}\sum_{s\in\mathcal{S}_1\cup\mathcal{S}_2}V\left(|D_s^+z(x)|\right).$$

The force at atom x is defined by

$$\mathcal{F}_{\rm qc}[z](x)\equiv-\frac{\partial E_{\rm qc}^{\rm tot}}{\partial z(x)}.$$

Since we only concern the influence of the ghost force, following [20], we assume that the interaction potential is harmonic, i.e.,

$$V_0(r)=\frac{1}{2}r^2,$$

where r is the distance between the atoms. Denote $\bar{r}=r/\varepsilon$, and we rescale the potential V_0 as $V(\bar{r})=V_0(r)$ with ε the equilibrium bond length.

Without taking into account the external force, we write the equilibrium equations for the QC approximation as

$$\mathcal{F}_{\rm qc}[z](x)=0$$

with

$$\mathcal{F}_{\rm qc}[z](x)=-12z(x)+\sum_{i=1}^{12}z(x+\varepsilon s_i),\qquad x\in\Omega_\varepsilon, x_1\leq-2\varepsilon,$$
$$\mathcal{F}_{\rm qc}[z](x)=-24z(x)+4\sum_{i=1}^{6}z(x+\varepsilon s_i),\qquad x\in\Omega_\varepsilon, x_1\geq 2\varepsilon.$$

For $x=(-\varepsilon,x_2)$,

$$\mathcal{F}_{\rm qc}[z](x)=-\frac{49}{2}z(x)+4\sum_{i=1}^{6}z(x+\varepsilon s_i)+\frac{1}{2}z(x+\varepsilon s_{12}).$$

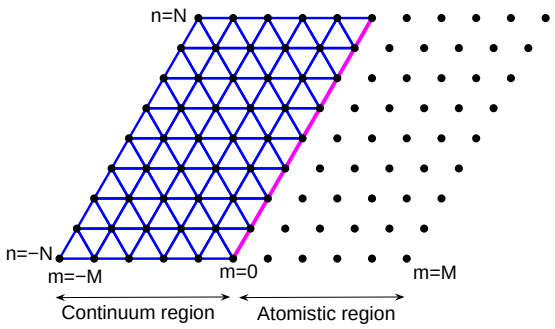

Fig. 2.2. Schematic picture of Ω_ε.

For $x = (0, x_2)$,

$$\mathcal{F}_{\rm qc}[z](x) = -18z(x) + [z(x+\varepsilon s_1) + z(x+\varepsilon s_6)] + \frac{5}{2}\Big(z(x+\varepsilon s_2) + z(x+\varepsilon s_5)\Big) + 4\Big(z(x+\varepsilon s_3) + z(x+\varepsilon s_4)\Big) + \Big(z(x+\varepsilon s_7) + z(x+\varepsilon s_{11}) + z(x+\varepsilon s_{12})\Big).$$

For $x = (\varepsilon, x_2)$,

$$\mathcal{F}_{\rm qc}[z](x) = -\frac{23}{2}z(x) + \sum_{i=1}^{12} z(x+\varepsilon s_i) - \frac{1}{2}z(x+\varepsilon s_9).$$

At the equilibrium state, we evaluate $\mathcal{F}_{\rm qc}$ at $z(x) = x$ to get

$$\mathcal{F}_{\rm qc}[x](x) = \begin{cases} (-3\varepsilon/4, \sqrt{3}\varepsilon/4), & \text{if} \quad x_1 = -\varepsilon, \\ (3\varepsilon/2, -\sqrt{3}\varepsilon/2), & \text{if} \quad x_1 = 0, \\ (-3\varepsilon/4, \sqrt{3}\varepsilon/4), & \text{if} \quad x_1 = \varepsilon, \\ (0,0), & \text{otherwise.} \end{cases}$$

The above equations imply $z_1(x) = -\sqrt{3}z_2(x)$. Therefore, we only study the first component of $z(x)$ and neglect the subscript if no confusion will occur. We denote the error caused by the ghost force by $y(x) \equiv z(x) - x$, which satisfies

$$\mathcal{F}_{\rm qc}[y](x) = \mathcal{F}_{\rm qc}[z](x) - \mathcal{F}_{\rm qc}[x](x) = -\mathcal{F}_{\rm qc}[x](x) \equiv f(x) \tag{2.3a}$$

with

$$f(x) = \begin{cases} 3\varepsilon/4, & \text{if} \quad x_1 = -\varepsilon, \\ -3\varepsilon/2, & \text{if} \quad x_1 = 0, \\ 3\varepsilon/4, & \text{if} \quad x_1 = \varepsilon, \\ 0 & \text{otherwise.} \end{cases} \tag{2.3b}$$

Boundary conditions need to be supplemented to close the system of equilibrium equations. Two types of boundary conditions will be considered in this paper. One is the periodic boundary condition in x_2 direction while homogeneous Dirichlet boundary condition in x_1 direction, which will be called periodic boundary condition if no confusion will occur. The other is the homogeneous Dirichlet boundary conditions in both x_1 and x_2 directions.

In what follows, we shall use a conventional notation $y(m,n) = y(x)$ with $x = \varepsilon(ma_1 + na_2)$, and call (2.3) the triangular lattice model with a QC approximation.

2.2. Periodic boundary condition

The periodic boundary condition can be written as

$$\begin{cases} y(-M,n) = y(M,n) = y(M+1,n) = 0, & n = -N, \cdots, N, \\ y(m,n) = y(m,2N+n), & m = -M, \cdots, M, n = -N, \cdots, N. \end{cases}$$

Observe that the solution of (2.3) with the periodic boundary condition takes a special form:

$$y(x) = cy(x_1),$$

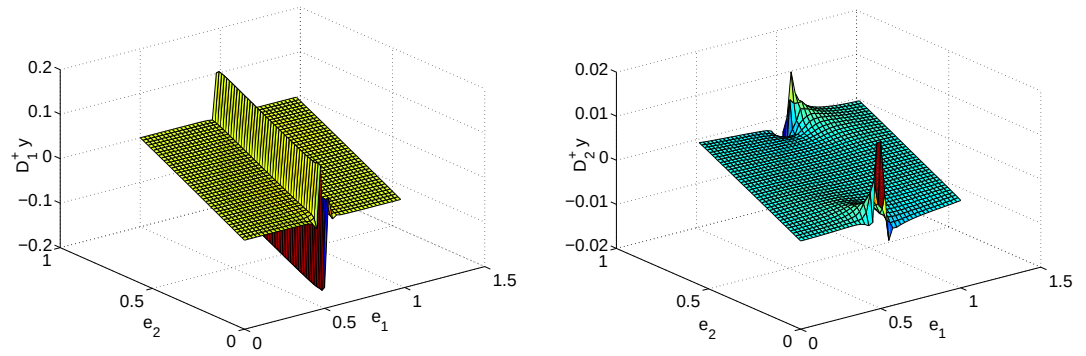

(a) $D_{s_1}^+ y$ (b) $D_{s_2}^+ y$

Fig. 2.3. Profiles of the discrete gradients for triangular lattice model with $M = N = 20$ under Dirichlet boundary condition.

namely, the solution is constant along x_2 direction. Based on this observation, we conclude that the QC approximation with the periodic boundary condition reduces to a one-dimensional problem. The equilibrium equations satisfied by $y(x_1)$ are as follows. In the continuum region, i.e., $m = -M + 1, \cdots, -2$,

$$8y(m+1) - 16y(m) + 8y(m-1) = 0,$$

and in the atomistic region, i.e., $m = 2, \cdots, M-1$,

$$y(m+2) + 4y(m+1) - 10y(m) + 4y(m-1) + y(m-2) = 0.$$

The equations in the interfacial region are

$$\begin{aligned}
&\frac{1}{2}y(1) + 8y(0) - \frac{33}{2}y(-1) + 8y(-2) = \frac{3}{4}\varepsilon,\\
&y(2) + 4y(1) - 13y(0) + 8y(-1) = -\frac{3}{2}\varepsilon,\\
&y(3) + 4y(2) - \frac{19}{2}y(1) + 4y(0) + \frac{1}{2}y(-1) = \frac{3}{4}\varepsilon.
\end{aligned}$$

The boundary condition is

$$y(-M) = y(M) = y(M+1) = 0.$$

The above equilibrium equations can also be obtained by considering a one-dimensional chain interacted with the following harmonic potential:

$$V(\{y\}) = \frac{k_1}{2}\sum_{|i-j|=1}|y_i - y_j|^2 + \frac{k_2}{2}\sum_{|i-j|=2}|y_i - y_j|^2 \tag{2.4}$$

with $k_1 = 4$ and $k_2 = 1$. This is the model studied in [2].

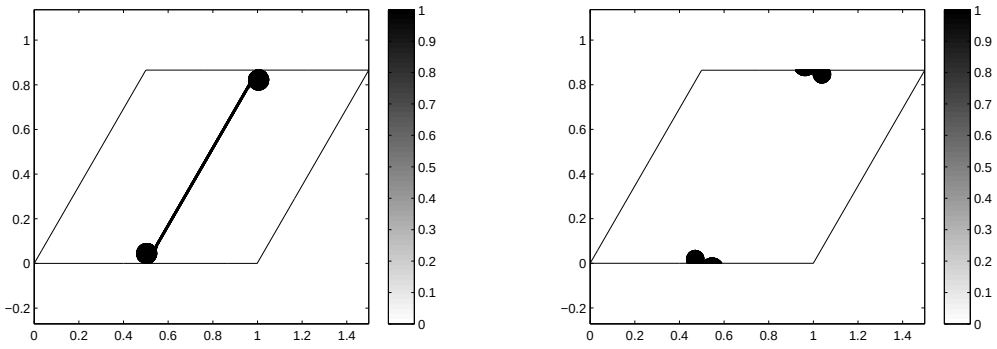

(a) $\chi_{E_1}(x)$ (b) $\chi_{E_2}(x)$

Fig. 2.4. Profiles of the characteristic functions for triangular lattice model.

2.3. Dirichlet boundary condition

The Dirichlet boundary condition can be written as

$$\begin{cases} y(-M,n) = y(M,n) = y(M+1,n) = 0, & n = -N,\cdots,N, \\ y(m,-N) = y(m,N) = 0, & m = -M,\cdots,-1, \\ y(m,-N-1) = y(m,-N) = y(m,N) = y(m,N+1) = 0, & m = 0,\cdots,M. \end{cases}$$

This boundary condition together with (2.3) yields an essentially two-dimensional model. We show profiles of discrete gradients $D^+_{s_1}y$ and $D^+_{s_2}y$ in Fig. 2.3 with $M = N = 20$. The profile of $D^+_{s_1}y$ is similar to that of the one-dimensional problem, but there is some difference if one zooms the interface. For $i = 1, 2$, we define

$$E_i = \Big\{ x \in \Omega_\varepsilon \mid |D_{s_i} y(x)| \geq c_0 \Big\},$$

and let χ_{E_i} be the characteristic function. Here c_0 is an empirical parameter chosen to highlight the interface. We plot χ_{E_i} in Fig. 2.4 with $M = N = 640$ and $c_0 = 10^{-3}$. In Fig. 2.4(a), the width of the interface near the boundary is much wider than that in the interior domain. No interfacial layer for $D^+_{s_2}y$ is observed in Fig. 2.4(b). Therefore, we only measure the width of

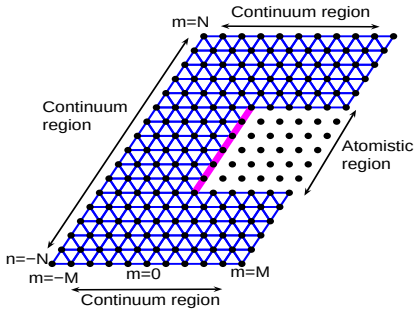

Fig. 2.5. Padding technique to remove the boundary effect.

Table 2.1: Width of the interfacial layer versus the equilibrium bond length ε for the triangular lattice model with Dirichlet boundary condition.

$\varepsilon\ (5\times 10^{-2})$	2^0	2^{-1}	2^{-2}	2^{-3}	2^{-4}	2^{-5}	Rate
Layer width(10^{-1})	5.0	2.3	1.1	0.56	0.28	0.14	1.02

Table 2.2: Width of the interfacial layer versus the equilibrium bond length ε by removing the effect of the boundary condition.

$\varepsilon(10^{-2})$	1.7	0.83	0.41	0.21	0.10	Rate
Layer width(10^{-2})	17	8.3	4.2	2.1	1.0	1.00

the interfacial layer for $D_{s_1}^+ y$, which is defined by

$$\max_n \Big\{ [m_1(n) - m_2(n)]\varepsilon \Big|\ m_1(n) = \text{argmax}_m\{x = ma_1\varepsilon + na_2\varepsilon \in E_1\} \\ m_2(n) = \text{argmin}_m\{x = ma_1\varepsilon + na_2\varepsilon \in E_1\} \Big\}.$$

Numerical results in Table 2.1 imply that the width of the interfacial layer scales $\mathcal{O}(\varepsilon)$.

One may doubt the above result could be caused by the boundary condition instead of the ghost force. To clarify this issue, we enlarge the continuum region to weaken the influence of the boundary condition. We set $N = 3M$ and use different equilibrium equations for different regions as in Fig. 2.5.

We plot $D_{s_1}^+ y$, $D_{s_2}^+ y$, and their characteristic functions in Fig. 2.6 and Fig. 2.7, which are similar to those in Fig. 2.3 and Fig. 2.4. The discrete gradients of the error are still localized around the interface, and are away from boundaries we imposed. This suggests that the interface is caused by the ghost force instead of the boundaries.

Table 2.2 shows the width of the interfacial layer in terms of ε. Numerical results suggest that the width of the interfacial layer is still of $\mathcal{O}(\varepsilon)$, which is consistent with that in Table 2.1.

The QC approximation discussed in this section is quite realistic except the potential function, which however seems enough to characterize the influence of the ghost force. Unfortu-

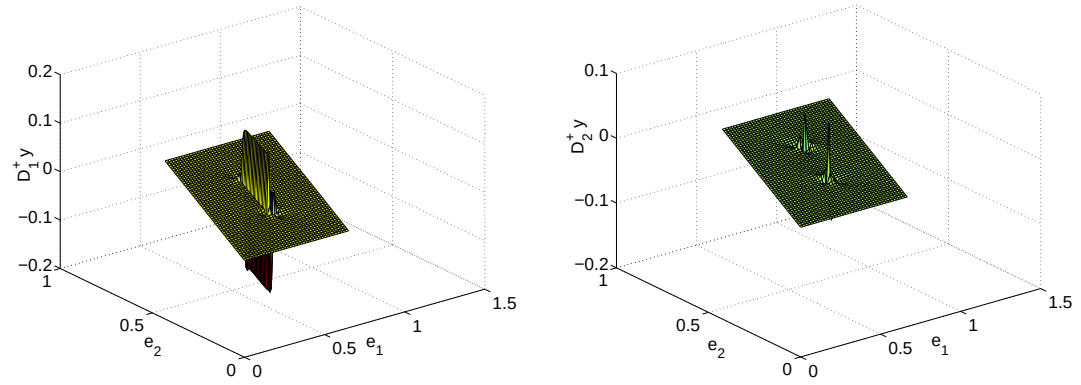

(a) $D_{s_1}^+ y$ (b) $D_{s_2}^+ y$

Fig. 2.6. Profiles of the discrete gradients for triangular lattice model with $M = 20$ and padding technique under Dirichlet boundary condition.

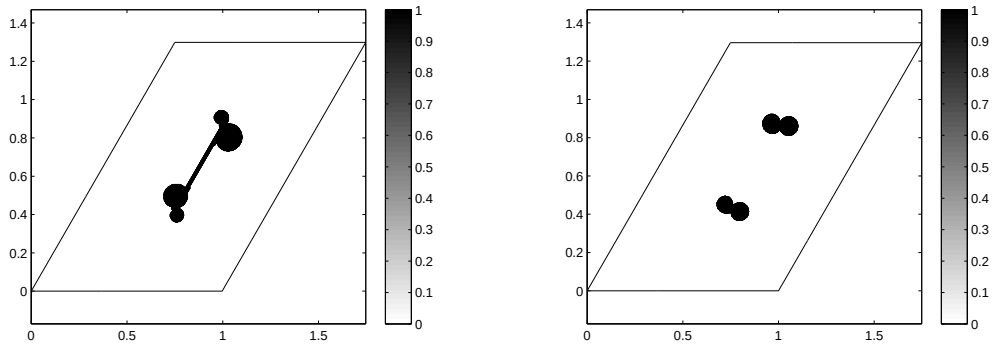

(a) $\chi_{E_1}(x)$ (b) $\chi_{E_2}(x)$

Fig. 2.7. Profiles of the characteristic functions for triangular lattice model with padding technique.

nately, it does not seem easy to solve this model analytically as we have done in [20] for the one-dimensional problem. In next section, we introduce a QC method for square lattice model that can be solved *analytically*. We shall prove that this square lattice model with the QC approximation does capture the main feature of the ghost force for the triangular lattice model with a planar interface.

3. A QC Method for Square Lattice

We consider the square lattice model with the harmonic potential. Compared to the standard interaction range of the square lattice, we assume a special interaction range as shown in Fig. 3.1 (Left). Namely, the first and second neighborhood interactions in x_1 direction, and the first neighborhood interaction in x_2 direction are taken into account. This seemingly strange selection may be obtained from a rotated triangular lattice as in Fig. 3.1 (Right). If we condense the interaction of the atoms $9, 4, 5, 11$ into one atom, and the atoms $8, 2, 1, 12$ into another, then we obtain a square lattice model with the special interaction range described above, which may be the underlying reason why it can be regarded as a *surrogate* model. We shall show in the next two sections that this model not only captures the main features of the triangular lattice model with the QC approximation as shown in Fig. 2.2, but also lends itself theoretically tractable.

Proceeding along the same line that leads to (2.3), we obtain the equilibrium equations for the error $y(x)$.[1)] In the continuum region, i.e., $m = -M, \cdots, -2$ and $n = -N, \cdots, N$,

$$12y_i(m,n) - y_i(m,n-1) - y_i(m,n+1) - 5y_i(m-1,n) - 5y_i(m+1,n) = 0, \tag{3.1}$$

for $i = 1, 2$, and in the atomistic region, i.e., $m = 2, \cdots, M$ and $n = -N, \cdots, N$,

$$\begin{aligned} 6y_i(m,n) - y_i(m,n-1) - y_i(m,n+1) - y_i(m-1,n) - y_i(m+1,n) \\ - y_i(m-2,n) - y_i(m+2,n) = 0, \quad i = 1, 2. \end{aligned} \tag{3.2}$$

The interface between the continuum model and the atomistic model is the line $m = 0$ as shown in Fig. 3.2, and M is assumed to be even for simplicity. The equilibrium equations for the layers $m = -1, 0$ and 1 are as follows.

[1)] We actually multiply -1 on both sides of (2.3).

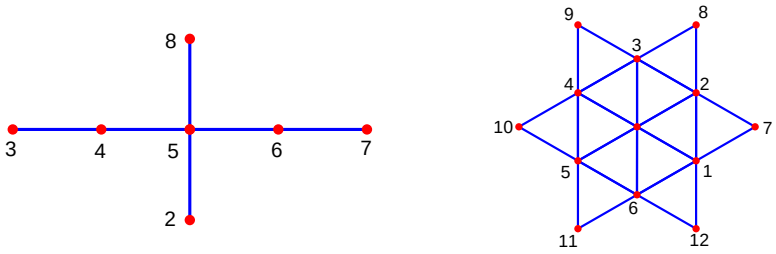

Fig. 3.1. Interaction ranges. Left: First and second neighborhood interactions in x_1 direction and first neighborhood interaction in x_2 direction for square lattice; Right: First and second neighborhood interactions for triangular lattice in a rotated coordinate.

For layer $m = -1$ and $n = -N, \cdots, N$,

$$\frac{25}{2}y_i(-1,n) - y_i(-1,n-1) - y_i(-1,n+1) - 5y_i(-2,n) - 5y_i(0,n) - \frac{1}{2}y_i(1,n) = f_i, \quad i = 1,2, \tag{3.3}$$

where $f_1 = -\varepsilon$ and $f_2 = 0$. For layer $m = 0$ and $n = -N, \cdots, N$,

$$9y_i(0,n) - y_i(0,n-1) - y_i(0,n+1) - 5y_i(-1,n) - y_i(1,n) - y_i(2,n) = f_i, \tag{3.4}$$

for $i = 1, 2$, where $f_1 = 2\varepsilon$ and $f_2 = 0$. For layer $m = 1$ and $n = -N, \cdots, N$,

$$\frac{11}{2}y_i(1,n) - y_i(1,n-1) - y_i(1,n+1) - y_i(0,n) - y_i(2,n) - \frac{1}{2}y_i(-1,n) - y_i(3,n) = f_i, \quad i = 1,2, \tag{3.5}$$

where $f_1 = -\varepsilon$ and $f_2 = 0$. Using $f_2 = 0$, we obtain $y_2 = 0$. We only consider y_1 and omit the subscript from now on.

First we impose the Dirichlet boundary condition in the x_1 direction, and the periodic

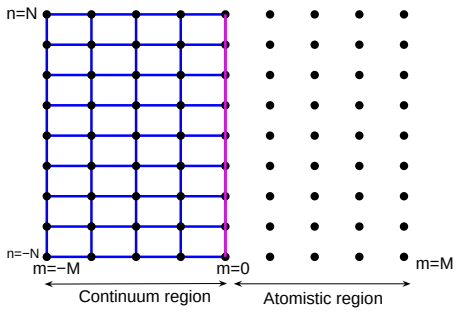

Fig. 3.2. Square lattice with a planar interface.

Table 3.1: Width of interfacial layer versus the equilibrium bond length ε for square lattice model.

ε (5×10^{-2})	2^0	2^{-1}	2^{-2}	2^{-3}	2^{-4}	Rate
Layer width (10^{-1})	10	5.5	2.4	1.2	0.59	1.04

Table 3.2: Width of the interfacial layer versus the equilibrium bond length ε by removing the effect of the boundary condition for the square lattice model.

$\varepsilon(10^{-2})$	3.3	1.7	0.83	0.41	0.21	Rate
Layer width(10^{-2})	13.3	6.7	4.4	1.7	0.83	1.00

boundary condition in the x_2 direction as

$$\begin{cases} y(-M,n)=y(M,n)=y(M+1,n)=0, \quad n=-N,\cdots,N, \\ y(m,n)=y(m,n+2N), \quad m=-M,\cdots,M, \ \ n=-N,\cdots,N. \end{cases} \tag{3.6}$$

Similar to the triangular lattice model, it is easy to check that this square lattice model reduces to a one-dimensional chain model with the following equilibrium equations and boundary conditions.

$$\begin{aligned} &5y(m+1)-10y(m)+5y(m-1)=0, && m=-M+1,\cdots,-2, \\ &y(m+2)+y(m+1)-4y(m)+y(m-1)+y(m-2)=0, && m=2,\cdots,M-1. \end{aligned}$$

The equations for the interface are

$$\begin{cases} \dfrac{1}{2}y(1)+5y(0)-\dfrac{21}{2}y(-1)+5y(-2)=\varepsilon, \\ y(2)+y(1)-7y(0)+5y(-1)=-2\varepsilon, \\ y(3)+y(2)-\dfrac{7}{2}y(1)+y(0)+\dfrac{1}{2}y(-1)=\varepsilon. \end{cases}$$

The boundary condition is

$$y(-M)=y(M)=y(M+1)=0.$$

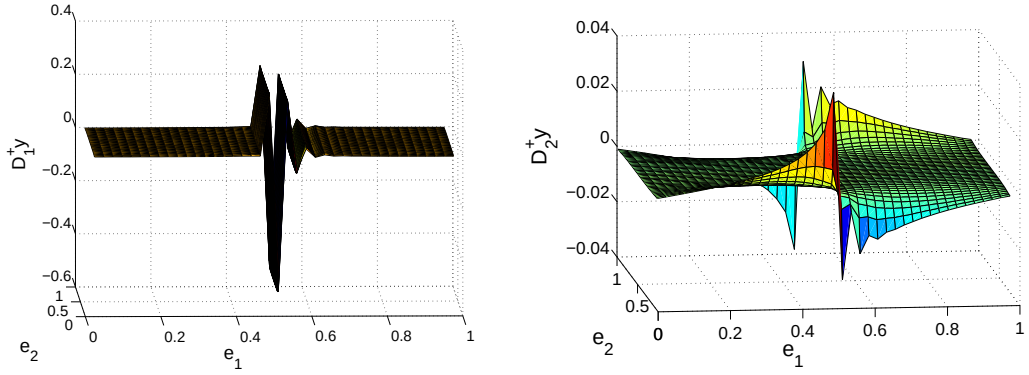

(a) $D_{s_1}^{+}y$ (b) $D_{s_2}^{+}y$

Fig. 3.3. Profiles of the discrete gradients of y for square lattice modle with $M=N=20$ under Dirichlet boundary condition.

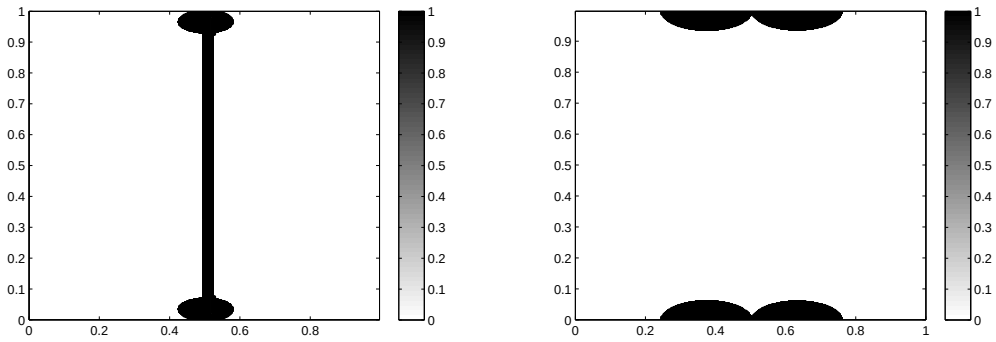

(a) $\chi_{E_1}(x)$ (b) $\chi_{E_2}(x)$

Fig. 3.4. Profiles of the characteristic functions for square lattice model.

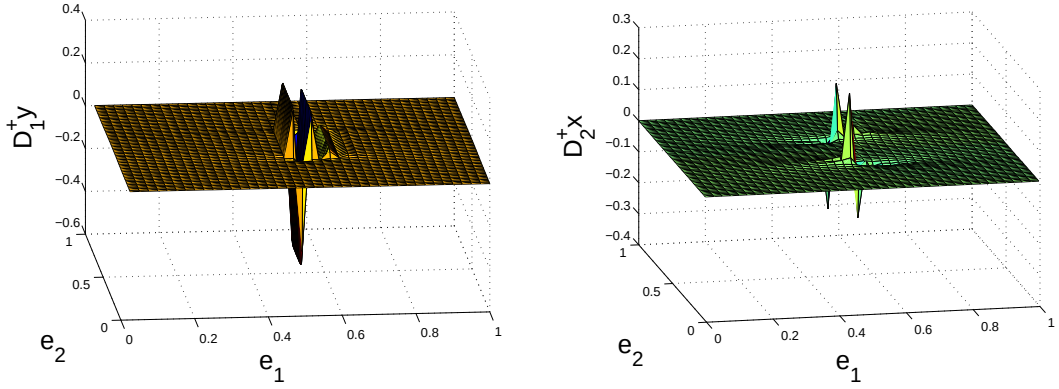

(a) $D_{s_1}^{+}y$ (b) $D_{s_2}^{+}y$

Fig. 3.5. Profiles of the discrete gradients for the square lattice model with $M = 20$ and padding technique under Dirichlet boundary condition.

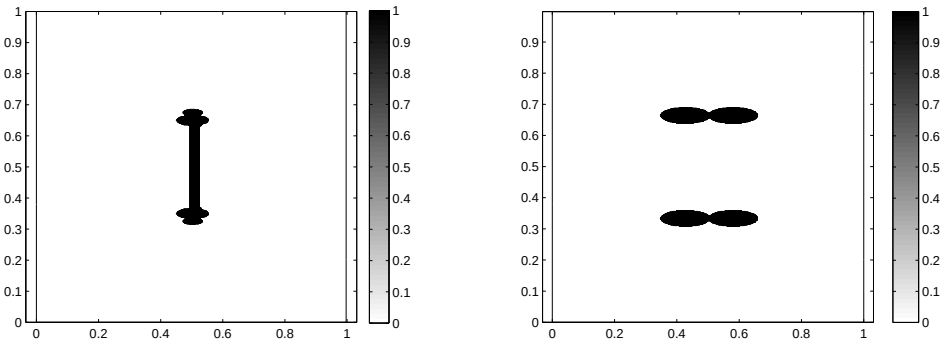

(a) $\chi_{E_1}(x)$ (b) $\chi_{E_2}(x)$

Fig. 3.6. Profiles of the characteristic functions for the square lattice model with padding technique.

It is clear that the above model is exactly the same as that has been studied in [20], which can also be obtained from the one-dimensional model (2.4) with $k_1 = k_2 = 1$.

Next we impose the Dirichlet boundary condition in both x_1 and x_2 directions.

$$\begin{cases} y(-M,n) = y(M,n) = y(M+1,n) = 0, & n = -N,\cdots,N, \\ y(m,-N) = y(m,N) = 0, & m = -M,\cdots,M. \end{cases} \tag{3.7}$$

Choosing $M = N = 20$, we show the profiles of the discrete gradients $D^+_{s_1}y$ and $D^+_{s_2}y$ in Fig. 3.3. The feature is similar to that of the triangular lattice model. To highlight the interface, we plot the characteristic functions χ_{E_1} and χ_{E_2} in Fig. 3.4 with $M = N = 320$ and $c_0 = 10^{-3}$.

We report the width of the interfacial layer in Table 3.1. It is clear that the width of the interfacial layer is of $\mathcal{O}(\varepsilon)$, which is the same with that of the triangular lattice model. In § 5, we shall prove this fact.

To clarify that the above result is caused by the ghost force instead of the boundary condition, we use the same setup shown in Fig. 2.5 for the square lattice model with a QC approximation. We plot the discrete gradients $D^+_{s_1}y$, $D^+_{s_2}y$, and their characteristic functions in Fig. 3.5 and Fig. 3.6. The profiles are similar to those in Fig. 3.3 and Fig. 3.4. The discrete gradients of the error are still localized around the interface, and are away from the boundaries.

Table 3.2 shows the width of the interfacial layer in terms of ε, which suggest that the width of the interfacial layer is still of $\mathcal{O}(\varepsilon)$. This is consistent with that in Table 3.1.

4. Exact Solution for the Square Lattice Model

To find the exact solution of the QC approximation (3.1) –(3.5) with Dirichlet boundary condition (3.7), we follow the approach in [20]: firstly, we find the general expression for the solution of the continuum equation and the atomistic equation by separation of variables ansatz, with certain unspecified constants; secondly, we use the equations around the interface to determine these constants. The next lemma gives the general expression of the solution.

Lemma 4.1. *For $m = -M,\cdots,-1$ and $n = -N,\cdots,N$, we have*

$$y(m,n) = \sum_{k=1}^{2N-1} a_k \sinh\Big((M+m)\alpha_k\Big) \sin\frac{k\pi}{2N}(N+n), \tag{4.1a}$$

where

$$\cosh\alpha_k = 1 + \frac{\lambda_k}{5}, \qquad \lambda_k = 2\sin^2\frac{k\pi}{4N}. \tag{4.1b}$$

For $m = 0,\cdots,M$ and $n = -N,\cdots,N$, we have

$$y(m,n) = \sum_{k=1}^{2N-1} \Big(b_k(-1)^m F_m(\gamma_k,\delta_k) + c_k f_m(\gamma_k,\delta_k)\Big) \sin\frac{k\pi}{2N}(N+n), \tag{4.2}$$

where

$$\cosh\gamma_k = \frac{1+\sqrt{25+8\lambda_k}}{4}, \quad \cosh\delta_k = \frac{-1+\sqrt{25+8\lambda_k}}{4}, \tag{4.3}$$

and

$$\begin{cases} F_m(\gamma,\delta) = \dfrac{\sinh[(M+1-m)\gamma] + \sinh[(M-m)\gamma]\cosh\delta}{\cosh\gamma+\cosh\delta} \\ \qquad\qquad - (-1)^m \dfrac{\cosh[(M-m)\delta]\sinh\gamma}{\cosh\gamma+\cosh\delta}, \\ f_m(\gamma,\delta) = F_m(\delta,\gamma). \end{cases} \tag{4.4}$$

The coefficients b_k and c_k are parameters to be determined; see (4.13).

Proof. By separation of variables, we get (4.1a).

The explicit expression for the solution of the atomistic model can also be obtained by separation of variables ansatz. Substituting $y(m,n) = f(m)g(n)$ into (3.2), we get

$$\sum_{i=-2}^{2}\Big(f(m+i)-f(m)\Big)g(n)+\sum_{i=-1}^{1}\Big(g(n+i)-g(n)\Big)f(m)=0.$$

By (3.7), we have

$$g(-N)=g(N)=0 \quad \text{and} \quad f(M)=f(M+1)=0.$$

We write the above equation as

$$\frac{1}{f(m)}\sum_{i=-2}^{2}\Big(f(m+i)-f(m)\Big)+\frac{1}{g(n)}\sum_{i=-1}^{1}\Big(g(n+i)-g(n)\Big)=0.$$

For $\lambda\in\mathbb{R}$, we get

$$\begin{cases} g(n+1)+(2\lambda-2)g(n)+g(n-1)=0,\\ f(m+2)+f(m+1)-(4+2\lambda)f(m)+f(m-1)+f(m-2)=0. \end{cases}$$

Using the boundary condition for g, i.e., $g(N)=g(-N)=0$, we have, for any $c\in\mathbb{R}$,

$$g(n)=c\sin\frac{k\pi}{2N}(n+N) \quad \text{and} \quad \lambda=2\sin^2\frac{k\pi}{4N}.$$

The characteristic equation for $f(m)$ is:

$$t^2+t^{-2}+t+t^{-1}-2(\lambda+2)=0.$$

Denote the roots of the above equation by $t_1,\cdots,t_4$. It is clear that

$$t_1=-e^{\gamma},\ t_2=-e^{-\gamma},\ t_3=e^{\delta},\ t_4=e^{-\delta},$$

with

$$2\cosh\gamma=-s_1,\quad s_1=\frac{-1-\sqrt{25+8\lambda}}{2},$$
$$2\cosh\delta=s_2,\qquad s_2=\frac{-1+\sqrt{25+8\lambda}}{2}.$$

This leads to

$$f(m)=a\big(-1\big)^m\sinh\Big((M-m)\gamma\Big)+b\big(-1\big)^m\cosh\Big((M-m)\gamma\Big)$$
$$+c\sinh\Big((M-m)\delta\Big)+d\cosh\Big((M-m)\delta\Big)$$

with constants a,b,c and d that will be determined by the conditions $f(M)=f(M+1)=0$. Since M is even, by $f(M)=0$, we obtain $b=-d$. By $f(M+1)=0$, we obtain

$$a\sinh\gamma-c\sinh\delta-b(\cosh\gamma+\cos\delta)=0.$$

Therefore,

$$b = \frac{a\sinh\gamma - c\sinh\delta}{\cosh\gamma + \cosh\delta}.$$

We write $f(m)$ as

$$f(m) = a\big(-1\big)^m \sinh\Big((M-m)\gamma\Big) + c\sinh\Big((M-m)\delta\Big) + \frac{a\sinh\gamma - c\sinh\delta}{\cosh\gamma+\cosh\delta}\Big\{\big(-1\big)^m\cosh\Big((M-m)\gamma\Big) - \cosh\Big((M-m)\delta\Big)\Big\}.$$

It is easy to rewrite $f(m)$ into a symmetrical form

$$f(m) = a\big(-1\big)^m F_m(\gamma,\delta) + cF_m(\delta,\gamma),$$

where $F_m(\gamma,\delta)$ is given in (4.4), this gives (4.3). □

Remark 4.1. The exact solution based on the series expansion is common in solving a finite difference equation. We refer to [17] and [11] for a thorough discussion.

Next we use the interfacial equations (3.3) – (3.5) to determine the coefficients a_k, b_k and c_k. Denote

$$y_{\rm cb}(m,n) = y(m,n) \qquad -M \le m \le -1, -N \le n \le N$$

with $y(m,n)$ given by (4.1a), and

$$y_{\rm at}(m,n) = y(m,n) \qquad 0 \le m \le M, -N \le n \le N$$

with $y(m,n)$ given by (4.2). Though $y_{\rm cb}$ and $y_{\rm at}$ are only defined in a subset of $\mathbb{Z}^2$, they can be extended to $\mathbb{Z}^2$, and satisfy

$$\mathcal{F}_\varepsilon[y_{\rm cb}](m,n) = 0, \qquad \mathcal{F}_{\rm at}[y_{\rm at}](m,n) = 0, \tag{4.5}$$

where

$$\begin{aligned}\mathcal{F}_\varepsilon[y](m,n) &\equiv 12y(m,n) - y(m,n-1) - y(m,n+1) - 5y(m-1,n) - 5y(m+1,n),\\ \mathcal{F}_{\rm at}[y](m,n) &\equiv 6y(m,n) - y(m,n-1) - y(m,n+1) - y(m-1,n) - y(m+1,n)\\ &\quad - y(m-2,n) - y(m+2,n).\end{aligned}$$

This observation is crucial to simplify the equations around the interface.

The equation for $m=-1$ changes to

$$\mathcal{F}_\varepsilon[y_{\rm cb}(\bar1,n)] + 5(y_{\rm cb}-y_{\rm at})(0,n) + \frac12\Big(y_{\rm cb}(\bar1,n) - y_{\rm at}(1,n)\Big) = -\varepsilon.$$

Using $\mathcal{F}_\varepsilon[y_{\rm cb}(\bar1,n)] = 0$, we have

$$5(y_{\rm cb}-y_{\rm at})(0,n) + \frac12\Big(y_{\rm cb}(\bar1,n) - y_{\rm at}(1,n)\Big) = -\varepsilon. \tag{4.6}$$

Proceeding in the same fashion, we get

$$y_{\rm at}(\bar1,n) - \frac12 y_{\rm at}(1,n) - \frac12 y_{\rm cb}(\bar1,n) = -\varepsilon, \tag{4.7}$$

$$3y_{\rm at}(0,n) + y_{\rm at}(\bar1,n) + y_{\rm at}(\bar2,n) - 5y_{\rm cb}(\bar1,n) = 2\varepsilon. \tag{4.8}$$

In what follows, we use the above simplified interfacial equations and the representation formulas to determine a_k, b_k and c_k. Subtracting (4.7) from (4.6), we obtain

$$5y_{\rm cb}(0,n)+y_{\rm cb}(\bar{1},n)=5y_{\rm at}(0,n)+y_{\rm at}(\bar{1},n).$$

Substituting (4.1a) and (4.2) into the above equation, we get

$$a_k=\frac{b_k(5F_0-F_{\bar{1}})(\gamma_k,\delta_k)+c_k(5f_0+f_{\bar{1}})(\gamma_k,\delta_k)}{5\sinh[M\alpha_k]+\sinh[(M-1)\alpha_k]}. \tag{4.9}$$

Substituting (4.1a) and (4.2) into (4.7), we get

$$\sum_{k=1}^{2N-1}\ell_k\sin\left[\frac{k\pi}{2N}(n+N)\right]=-2\varepsilon$$

with

$$\ell_k=-\sinh[(M-1)\alpha_k]a_k+(-2F_{\bar{1}}+F_1)(\gamma_k,\delta_k)b_k+(2f_{\bar{1}}-f_1)(\gamma_k,\delta_k)c_k.$$

Using the discrete Fourier transform, we get

$$\ell_k=\frac{2\times(-2\varepsilon)}{2N-1+1}\sum_{j=1}^{2N-1}\sin\frac{k\pi j}{2N}=\begin{cases}-\dfrac{2\varepsilon}{N}\cot\dfrac{k\pi}{4N}, & \text{if } k \text{ is odd},\\ 0, & \text{if } k \text{ is even}.\end{cases}$$

This leads to

$$P_kb_k+p_kc_k=\ell_k, \tag{4.10}$$

where

$$P_k=[-2F_{\bar{1}}+F_1-\rho_k(-F_{\bar{1}}+5F_0)](\gamma_k,\delta_k), \tag{4.11a}$$

$$p_k=[2f_{\bar{1}}-f_1-\rho_k(f_{\bar{1}}+5f_0)](\gamma_k,\delta_k), \tag{4.11b}$$

$$\rho_k=\frac{\sinh[(M-1)\alpha_k]}{5\sinh[M\alpha_k]+\sinh[(M-1)\alpha_k]}. \tag{4.11c}$$

Using (4.7) and (4.8) to eliminate $y_{\rm cb}(\bar{1},n)$, we obtain

$$3y_{\rm at}(0,n)-9y_{\rm at}(\bar{1},n)+y_{\rm at}(\bar{2},n)+5y_{\rm at}(1,n)=12\varepsilon.$$

The coefficients b_k and c_k satisfy

$$R_kb_k+r_kc_k=-6\ell_k, \tag{4.12a}$$

where

$$\begin{cases}R_k=(3F_0+9F_{\bar{1}}+F_{\bar{2}}-5F_1)(\gamma_k,\delta_k),\\ r_k=(3f_0-9f_{\bar{1}}+f_{\bar{2}}+5f_1)(\gamma_k,\delta_k).\end{cases} \tag{4.12b}$$

To solve the linear system (4.10) and (4.12), we need to check whether $P_kr_k-p_kR_k$ is nonzero for all k. We shall prove in Lemma 5.4 that this is indeed the case. Therefore, we may solve (4.10) and (4.12) to obtain

$$b_k=\frac{r_k+6p_k}{P_kr_k-p_kR_k}\ell_k,\qquad c_k=-\frac{R_k+6P_k}{P_kr_k-p_kR_k}\ell_k. \tag{4.13}$$

Substituting the above equation into (4.9), we get

$$a_k = \frac{(r_k + 6p_k)(5F_0 - F_{\bar{1}})(\gamma_k, \delta_k) - (R_k + 6P_k)(5f_0 + f_{\bar{1}})(\gamma_k, \delta_k)}{(5\sinh[M\alpha_k] + \sinh[(M-1)\alpha_k])\big(P_k r_k - p_k R_k\big)}\ell_k.$$

To sum up, we obtain the representation formulas for the solution of the QC approximation by specifying the parameters a_k, b_k and c_k in Lemma 4.1.

Theorem 4.1. *Let y be the solution of problem* (3.1)-(3.5). *Then for $m = -M, \cdots, \bar{1}$ and $n = -N, \cdots, N$,*

$$y(m,n) = -\frac{2\varepsilon}{N}\sum_{\substack{k=1\\ k\ odd}}^{2N-1} \frac{\mathcal{Q}_k}{P_k r_k - R_k p_k}\frac{\sinh[(M+m)\alpha_k]}{\sinh[(M-1)\alpha_k]}\rho_k \cdot \cot\frac{k\pi}{4N}\sin\left[\frac{k\pi}{2N}(n+N)\right], \tag{4.14}$$

where ρ_k is given in (4.11c). *For $m = 0, \cdots, M$ and $n = -N, \cdots, N$,*

$$y(m,n) = -\frac{2\varepsilon}{N}\sum_{\substack{k=1\\ k\ odd}}^{2N-1} \frac{\mathcal{Q}_{m,k}}{P_k r_k - R_k p_k}\cot\frac{k\pi}{4N}\sin\left[\frac{k\pi}{2N}(n+N)\right], \tag{4.15}$$

where

$$\begin{aligned}
P_k r_k - R_k p_k &= 6(8\rho_k - 1)\begin{vmatrix} F_0 & -F_{\bar{1}} \\ f_0 & f_{\bar{1}} \end{vmatrix} + (25\rho_k - 3)\begin{vmatrix} -F_1 & F_0 \\ f_1 & f_0 \end{vmatrix} - \begin{vmatrix} -F_1 & F_{\bar{2}} \\ f_1 & f_{\bar{2}} \end{vmatrix} \\
&\quad + (2 - \rho_k)\begin{vmatrix} -F_{\bar{1}} & F_{\bar{2}} \\ f_{\bar{1}} & f_{\bar{2}} \end{vmatrix} + (5\rho_k - 1)\begin{vmatrix} -F_1 & -F_{\bar{1}} \\ f_1 & f_{\bar{1}} \end{vmatrix} - 5\rho_k\begin{vmatrix} F_0 & F_{\bar{2}} \\ f_0 & f_{\bar{2}} \end{vmatrix}, \\
\mathcal{Q}_k &= 12\begin{vmatrix} F_0 & -F_{\bar{1}} \\ f_0 & f_{\bar{1}} \end{vmatrix} + 5\begin{vmatrix} F_0 & F_{\bar{2}} + F_1 \\ f_0 & f_{\bar{2}} - f_1 \end{vmatrix} + \begin{vmatrix} -F_{\bar{1}} & F_{\bar{2}} + F_1 \\ f_{\bar{1}} & f_{\bar{2}} - f_1 \end{vmatrix},
\end{aligned}$$

and

$$\begin{aligned}
\mathcal{Q}_{m,k} &= 3(1 - 10\rho_k)\begin{vmatrix} (-1)^m F_m & F_0 \\ f_m & f_0 \end{vmatrix} \\
&\quad + 3(1 - 2\rho_k)\begin{vmatrix} (-1)^m F_m & -F_{\bar{1}} \\ f_m & f_{\bar{1}} \end{vmatrix} + \begin{vmatrix} (-1)^m F_m & F_{\bar{2}} + F_1 \\ f_m & f_{\bar{2}} - f_1 \end{vmatrix}.
\end{aligned}$$

As an immediate consequence of the above theorem, the solution is symmetrical with respect to $n = 0$, i.e.,

$$y(m,n) = y(m,-n), \tag{4.16}$$

which can be easily verified from the representation formulas (4.14) and (4.15).

5. Pointwise Estimate of the Error

The main result of this section is the pointwise estimate for the error caused by the ghost force of a QC method for square lattice introduced in § 3.

Theorem 5.1. *Let y be the solution of problem* (3.1)-(3.5). *Then*

$$|Dy(m,n)| \le \frac{C}{m^2}\exp\left[-\frac{|m|}{6\sqrt{5}N}\right], \quad m \le -1, \tag{5.1}$$

$$|Dy(m,n)| \le C\left(\left(\frac{3-\sqrt{5}}{2}\right)^m + \frac{1}{m^2+1}\exp\left[-\frac{2m}{15N}\right]\right), \quad m \ge 0. \tag{5.2}$$

The above result suggests that the error decays algebraically away from the interface.

Remark 5.1. The above theorem indicates that the width of the interface is of $\mathcal{O}(\varepsilon)$. It also suggests that the gradient of the error decays away from the interface to $\mathcal{O}(\varepsilon)$ at distance $\mathcal{O}(\sqrt{\varepsilon}\,)$, while for one-dimensional problem, the error decays away from the interface to $\mathcal{O}(\varepsilon)$ at distance $\mathcal{O}(\varepsilon|\ln\varepsilon|\,)$ as shown in [2, 20].

Remark 5.2. In view of the estimates (5.1) and (5.2), we conclude that the gradient of the solution actually decays as fast as $(m^2+1)^{-1}$, which is due to the decay properties of the lattice Green's function associated with $\mathcal{F}_{\rm qc}$. We shall elaborate on this issue in the future work.

5.1. Some lemmas

We exploit the explicit expression of the solution in Theorem 4.1 to prove Theorem 5.1. Note that the terms $P_k r_k - R_k p_k$, $\mathcal{Q}_k$ and $\mathcal{Q}_{m,k}$ consist of the terms like $(-1)^m F_m f_n - (-1)^n F_n f_m$ for different integers m and n. The asymptotical behavior of such terms will be given in a series of lemmas, i.e., Lemma 5.4, Lemma 5.5 and Lemma 5.6. We begin with certain elementary estimates that will be frequently used later on.

Lemma 5.1. *For $1 \le k \le 2N-1$, there holds*

$$\frac{\lambda_k}{6} \le \cosh\gamma_k - \frac{3}{2} \le \frac{\lambda_k}{5}, \tag{5.3}$$

$$\sinh\delta_k \ge \sqrt{\frac{\lambda_k}{3}}, \tag{5.4}$$

$$\sinh\alpha_k \ge \sqrt{\frac{2\lambda_k}{5}}, \quad \sinh\frac{\alpha_k}{2} = \sqrt{\frac{\lambda_k}{10}}. \tag{5.5}$$

Proof. Invoking (4.3), we have

$$\cosh\gamma_k - \frac{3}{2} = \frac{1}{4}\left(\sqrt{25+8\lambda_k}-5\right) = \frac{2\lambda_k}{\sqrt{25+8\lambda_k}+5},$$

which immediately implies (5.3). The estimate (5.5) follows from (4.1a) by definition. Using (4.3), we have

$$\cosh\gamma_k - \cosh\delta_k = \frac{1}{2}, \tag{5.6}$$

this implies

$$\begin{aligned}\sinh^2\delta_k &= \cosh^2\delta_k - 1 = (\cosh\gamma_k - 1/2)^2 - 1\\ &= (\cosh\gamma_k - 3/2 + 2)(\cosh\gamma_k - 3/2).\end{aligned}$$

Using (5.3), we have

$$\sinh^2\delta_k \ge 2(\cosh\gamma_k - 3/2) \ge \frac{\lambda_k}{3}.$$

This gives (5.4). □

To proceed further, we need the following estimates.

Lemma 5.2. *For $1 \le k \le 2N-1$, there holds*

$$\exp(-\alpha_k) \le \exp\Big[-\frac{k}{2\sqrt{5}N}\Big], \tag{5.7}$$

$$\exp(-\gamma_k) \le \frac{3-\sqrt{5}}{2}, \quad \exp(-\delta_k) \le \exp\Big[-\frac{k}{5N}\Big]. \tag{5.8}$$

Proof. We only prove (5.7). Other cases are similar. Using (5.5) and $\cosh\alpha_k \ge 1$, we have

$$\begin{aligned}\exp\alpha_k &= \cosh\alpha_k + \sinh\alpha_k \\ &\ge 1 + \sqrt{\frac{2\lambda_k}{5}} = 1 + \frac{2}{\sqrt{5}}\sin\frac{k\pi}{4N}.\end{aligned}$$

Using Jordan's inequality $\sin x \ge 2x/\pi$ for $x \in [0, \pi/2]$, we have

$$\exp\alpha_k \ge 1 + \frac{k}{\sqrt{5}N}.$$

For any $0 < x < 2/\sqrt{5}$, we have

$$\ln(1+x) \ge x(1-x/2) \ge x(1-1/\sqrt{5}) \ge x/2.$$

Using the fact that $k/(\sqrt{5}N) \le 2/\sqrt{5}$ since $1 \le k \le 2N-1$, and combining the above two inequalities, we obtain

$$\begin{aligned}\exp(-\alpha_k) &\le \left(1 + \frac{k}{\sqrt{5}N}\right)^{-1} = \exp[-\ln(1 + k/(\sqrt{5}N))] \\ &\le \exp\left[-\frac{k}{2\sqrt{5}N}\right].\end{aligned}$$

This completes the proof of the lemma. □

The next lemma concerns the estimate of ρ_k.

Lemma 5.3.

$$0 < 1 - 6\rho_k \le \frac{5}{6}\left(\frac{\lambda_k}{5} + \frac{1}{M-1} + \sinh\alpha_k\right). \tag{5.9}$$

Proof. Using the definition of ρ_k, we get

$$1 - 6\rho_k = \frac{5\,(\sinh[M\alpha_k] - \sinh[(M-1)\alpha_k])}{5\sinh[M\alpha_k] + \sinh[(M-1)\alpha_k]},$$

which implies the left hand side of (5.9). Moreover

$$\begin{aligned}1 - 6\rho_k &\le \frac{5}{6}\left(\frac{\sinh[M\alpha_k]}{\sinh[(M-1)\alpha_k]} - 1\right) \\ &= \frac{5}{6}\Big(\cosh\alpha_k - 1 + \cot[(M-1)\alpha_k]\sinh\alpha_k\Big).\end{aligned}$$

Using $\cosh t \le 1 + \sinh t$ for any $t \in \mathbb{R}$, we have

$$\begin{aligned}\cot[(M-1)\alpha_k]\sinh\alpha_k &\le \sinh\alpha_k + \frac{\sinh\alpha_k}{\sinh[(M-1)\alpha_k]} \\ &\le \sinh\alpha_k + \frac{1}{M-1},\end{aligned}$$

where we have used the elementary inequality

$$\frac{\sinh[Mt]}{\sinh t} \geq M.$$

Combining the above three inequalities, we obtain the right hand side of (5.9). □

By the definition of ρ_k and the left hand side of (5.9), we get

$$0 < \rho_k \leq 1/6. \tag{5.10}$$

A direct calculation gives

$$\begin{aligned}
&\Big(\cosh\gamma + \cosh\delta\Big)\Big((-1)^m F_m f_n - (-1)^n F_n f_m\Big) \\
&= A\sinh[M\gamma]\sinh[M\delta] + B\cosh[M\gamma]\sinh[M\delta] \\
&\quad + C\sinh[M\gamma]\cosh[M\delta] + D\cosh[M\gamma]\cosh[M\delta] \\
&\quad - \sinh[(m-n)\delta]\sinh\gamma + (-1)^{m+n}\sinh[(m-n)\gamma]\sinh\delta,
\end{aligned}$$

where

$$\begin{aligned}
A &= (-1)^m\cosh[m\gamma]\cosh[(n-1)\delta] + (-1)^m\cosh[n\delta]\cosh[(m-1)\gamma] \\
&\quad - (-1)^n\cosh[n\gamma]\cosh[(m-1)\delta] - (-1)^n\cosh[m\delta]\cosh[(n-1)\gamma], \\
B &= -(-1)^m\sinh[m\gamma]\cosh[(n-1)\delta] - (-1)^m\sinh[(m-1)\gamma]\cosh[n\delta] \\
&\quad + (-1)^n\sinh[n\gamma]\cosh[(m-1)\delta] + (-1)^n\sinh[(n-1)\gamma]\cosh[m\delta], \\
C &= -(-1)^m\cosh[m\gamma]\sinh[(n-1)\delta] - (-1)^m\cosh[(m-1)\gamma]\sinh[n\delta] \\
&\quad + (-1)^n\cosh[n\gamma]\sinh[(m-1)\delta] + (-1)^n\cosh[(n-1)\gamma]\sinh[m\delta], \\
D &= (-1)^m\sinh[m\gamma]\sinh[(n-1)\delta] + (-1)^m\sinh[(m-1)\gamma]\sinh[n\delta] \\
&\quad - (-1)^n\sinh[n\gamma]\sinh[(m-1)\delta] - (-1)^n\sinh[(n-1)\gamma]\sinh[m\delta].
\end{aligned}$$

The following lemma gives a lower bound for $|P_k r_k - R_k p_k|$.

Lemma 5.4. *There holds*

$$\Big(\cosh\gamma_k + \cosh\delta_k\Big)\Big|P_k r_k - R_k p_k\Big| \geq \frac{5}{24}\left(1 - \exp\left[-\frac{2M}{5N}\right]\right)\exp\left[M(\gamma_k + \delta_k)\right]. \tag{5.11}$$

Proof. A direct calculation gives

$$\begin{aligned}
&\Big(\cosh\gamma_k + \cosh\delta_k\Big)\Big(P_k r_k - R_k p_k\Big) \\
&= A_k\sinh[M\gamma_k]\sinh[M\delta_k] + B_k\cosh[M\gamma_k]\sinh[M\delta_k] \\
&\quad + C_k\sinh[M\gamma_k]\cosh[M\delta_k] + D_k\cosh[M\gamma_k]\cosh[M\delta_k] \\
&\quad + 2(12 + 2\lambda_k - 72\rho_k)\sinh\gamma_k\sinh\delta_k,
\end{aligned}$$

where

$$\begin{aligned}
A_k &= \left(4\lambda_k^2 + \frac{313}{2}\lambda_k + 315\right)\rho_k - 6\lambda_k^2 - 39\lambda_k - \frac{105}{2},\\
B_k &= \left(18\lambda_k + \frac{225}{4} + \left(\frac{229}{4} + 2\lambda_k\right)\sqrt{25+8\lambda_k}\right)\rho_k \sinh\gamma_k\\
&\quad + \left(\frac{25}{2} + 4\lambda_k - (14+4\lambda_k)\sqrt{25+8\lambda_k}\right)\sinh\gamma_k,\\
C_k &= \left(-18\lambda_k - \frac{225}{4} + \left(\frac{229}{4} + 2\lambda_k\right)\sqrt{25+8\lambda_k}\right)\rho_k \sinh\delta_k\\
&\quad + \left(-\frac{25}{2} - 4\lambda_k - (14+4\lambda_k)\sqrt{25+8\lambda_k}\right)\sinh\delta_k,\\
D_k &= \Big((169+8\lambda_k)\rho_k - (74+20\lambda_k)\Big)\sinh\gamma_k \sinh\delta_k.
\end{aligned}$$

Using (5.10), we may show that

$$A_k, B_k, C_k, D_k < 0. \tag{5.12}$$

Using $D_k < 0$ and invoking (5.10) once again, we have

$$\begin{aligned}
&D_k \cosh[M\gamma_k]\cosh[M\delta_k] + 2\Big(12 + 2\lambda_k - 72\rho_k\Big)\sinh\gamma_k \sinh\delta_k\\
&\le D_k + 2\Big(12 + 2\lambda_k - 72\rho_k\Big)\sinh\gamma_k \sinh\delta_k\\
&= \Big((169+8\lambda_k)\rho_k - (74+20\lambda_k) + 2(12 + 2\lambda_k - 72\rho_k)\Big)\sinh\gamma_k \sinh\delta_k\\
&= \Big((24+8\lambda_k)\rho_k - (50+16\lambda_k)\Big)\sinh\gamma_k \sinh\delta_k\\
&\le -\Big(46 + 44\lambda_k/3\Big)\sinh\gamma_k \sinh\delta_k < 0,
\end{aligned} \tag{5.13}$$

which together with (5.12) implies

$$(\cosh\gamma_k + \cosh\delta_k)(P_k r_k - R_k p_k) < 0.$$

Combining the above equation with (5.12) and (5.13), we obtain

$$\begin{aligned}
&\Big|(\cosh\gamma_k + \cosh\delta_k)(P_k r_k - R_k p_k)\Big|\\
&= -\Big(\cosh\gamma_k + \cosh\delta_k\Big)\Big(P_k r_k - R_k p_k\Big)\\
&= -B_k \cosh[M\gamma_k]\sinh[M\delta_k] - A_k \sinh[M\gamma_k]\sinh[M\delta_k] - C_k \sinh[M\gamma_k]\cosh[M\delta_k]\\
&\qquad + \Big(-D_k \cosh[M\gamma_k]\cosh[M\delta_k] - 2(12 + 2\lambda_k - 72\rho_k)\sinh\gamma_k \sinh\delta_k\Big)\\
&\ge |B_k| \cosh[M\gamma_k]\sinh[M\delta_k].
\end{aligned} \tag{5.14}$$

Using (5.9), we bound $|B_k|$ as

$$\begin{aligned}
|B_k| = -B_k &= -\left(18\lambda_k + \frac{225}{4} + \left(\frac{229}{4} + 2\lambda_k\right)\sqrt{25+8\lambda_k}\right)\rho_k \sinh\gamma_k\\
&\quad - \left(\frac{25}{2} + 4\lambda_k - (14+4\lambda_k)\sqrt{25+8\lambda_k}\right)\sinh\gamma_k\\
&\ge \left(\left(\frac{107}{24} + \frac{11}{3}\lambda_k\right)\sqrt{25+8\lambda_k} - \frac{175}{8} - 7\lambda_k\right)\sinh\gamma_k.
\end{aligned}$$

A direct calculation gives $\sinh\gamma_k \geq \sqrt{5}/2$, which together with the above inequality yields

$$|B_k| \geq \frac{5}{6}. \tag{5.15}$$

By (5.8), we have

$$\exp[2M\delta_k] \geq \exp[2kM/(5N)] \geq \exp[2M/(5N)].$$

It follows from the above inequality that

$$\begin{aligned}\sinh[M\delta_k] &= \frac{1}{2}\exp[M\delta_k]\,(1-\exp[-2M\delta_k]) \\ &\geq \frac{1}{2}\,(1-\exp[-2M/(5N)])\exp[M\delta_k].\end{aligned}$$

Substituting the above inequality and (5.15) into (5.14) implies (5.11). □

Next two lemmas concern the upper bounds of $\mathcal{Q}_k$ and $\mathcal{Q}_{m,k}$. Instead of calculating all the coefficients of $\mathcal{Q}_k$ and $\mathcal{Q}_{m,k}$ as we have done for $(\cosh\gamma_k+\cosh\delta_k)|P_kr_k-R_kp_k|$, we consider the coefficients of the leading order terms of $\mathcal{Q}_k$ and $\mathcal{Q}_{m,k}$. We write

$$\begin{aligned}&\Big(\cosh\gamma+\cosh\delta\Big)\Big((-1)^mF_mf_n-(-1)^nF_nf_m\Big)\\ =&\frac{1}{4}(A+B+C+D)e^{M(\gamma+\delta)}\frac{1}{4}(-A-B+C+D)e^{M(\gamma-\delta)}+\text{L.O.T.}\end{aligned} \tag{5.16a}$$

with

$$\begin{cases} A+B+C+D=(e^{\gamma}+e^{\delta})\left((-1)^me^{-(n\delta+m\gamma)}-(-1)^ne^{-(n\gamma+m\delta)}\right),\\ -A-B+C+D=(e^{\gamma}+e^{-\delta})\left(-(-1)^me^{n\delta-m\gamma}+(-1)^ne^{m\delta-n\gamma}\right),\end{cases} \tag{5.16b}$$

and L.O.T. stands for the terms that are of lower order than $e^{M(\gamma+\delta)}$ and $e^{M(\gamma-\delta)}$. Using (4.14), we write $(\cosh\gamma_k+\cosh\delta_k)\mathcal{Q}_k$ as

$$\Big(\cosh\gamma_k+\cosh\delta_k\Big)\mathcal{Q}_k=\mathcal{Q}_k^0\exp[M(\gamma_k+\delta_k)]+\mathcal{Q}_k^1\exp[M(\gamma_k-\delta_k)]+\text{L.O.T.} \tag{5.17a}$$

with

$$\begin{aligned}\mathcal{Q}_k^0=\frac{1}{4}\Big(e^{\gamma_k}+e^{\delta_k}\Big)\Big\{&12(e^{\gamma_k}+e^{\delta_k})+5(e^{2\delta_k}-e^{2\gamma_k})-5(e^{-\gamma_k}+e^{-\delta_k})\\ &-e^{\gamma_k+\delta_k}(e^{\gamma_k}+e^{\delta_k})+e^{\gamma_k-\delta_k}-e^{\delta_k-\gamma_k}\Big\},\end{aligned} \tag{5.17b}$$

$$\begin{aligned}\mathcal{Q}_k^1=\frac{1}{4}\Big(e^{\gamma_k}+e^{-\delta_k}\Big)\Big\{&-12(e^{\gamma_k}+e^{-\delta_k})+5(e^{2\gamma_k}-e^{-2\delta_k})+5(e^{-\gamma_k}+e^{\delta_k})\\ &+e^{\gamma_k-\delta_k}(e^{\gamma_k}+e^{-\delta_k})+e^{-\gamma_k-\delta_k}-e^{\gamma_k+\delta_k}\Big\}.\end{aligned} \tag{5.17c}$$

We have the following estimate for $\mathcal{Q}_k^0$ and $\mathcal{Q}_k^1$.

Lemma 5.5. *There exists C such that*

$$|\mathcal{Q}_k^0|+|\mathcal{Q}_k^1|\leq C\sqrt{\lambda_k}. \tag{5.18}$$

Proof. We only estimate $\mathcal{Q}_k^0$, and $\mathcal{Q}_k^1$ can be bounded similarly. We firstly write $\mathcal{Q}_k^0$ as

$$\mathcal{Q}_k^0 = \frac{1}{4}\Big(e^{\gamma_k}+e^{\delta_k}\Big)\Big\{(12+e^{-\delta_k}-e^{2\delta_k})e^{\gamma_k}-(5+e^{\delta_k})(e^{2\gamma_k}+e^{-\gamma_k}) + 12e^{\delta_k}-5e^{-\delta_k}+5e^{2\delta_k}\Big\}. \tag{5.19}$$

By definition, we have

$$\cosh[2\gamma_k] = 2\cosh^2\gamma_k - 1 = \cosh\gamma_k + \lambda_k + 2, \tag{5.20}$$

which implies

$$\begin{aligned} e^{2\gamma_k}+e^{-\gamma_k} &= \cosh[2\gamma_k]+\sinh[2\gamma_k]+\cosh\gamma_k-\sinh\gamma_k \\ &= 2\cosh\gamma_k+\lambda_k+2+\sinh\gamma_k(2\cosh\gamma_k-1) \\ &= 2(e^{\gamma_k}+1)+\lambda_k+\sinh\gamma_k(2\cosh\gamma_k-3). \end{aligned}$$

Substituting the above equation into (5.19) produces

$$\mathcal{Q}_k^0 = \frac{1}{4}\Big(e^{\gamma_k}+e^{\delta_k}\Big)\Big\{(5-e^{\gamma_k})[2(e^{\delta_k}-1)-e^{-\delta_k}+e^{2\delta_k})] - (5+e^{\delta_k})[\lambda_k+\sinh\gamma_k(2\cosh\gamma_k-3)]\Big\}.$$

Using (5.6), we get

$$2(e^{\delta_k}-1)-e^{-\delta_k}+e^{2\delta_k} = (e^{\delta_k}-1)(3+2\cosh\delta_k) = 2(\cosh\gamma_k+1)(e^{\delta_k}-1).$$

Combining the above two equations, we obtain

$$\mathcal{Q}_k^0 = (e^{\gamma_k}+e^{\delta_k})\Big\{2(5-e^{\gamma_k})(\cosh\gamma_k+1)(e^{\delta_k}-1) - (5+e^{\delta_k})[\lambda_k+\sinh\gamma_k(2\cosh\gamma_k-3)]\Big\}. \tag{5.21}$$

Proceeding along the same way that leads to (5.21), we obtain

$$\mathcal{Q}_k^1 = \frac{1}{4}(e^{\gamma_k}+e^{\delta_k})\Big\{(5+e^{-\delta_k})[\lambda_k+2\sinh\gamma_k(2\cosh\gamma_k-3)] + (5-e^{\gamma_k})(1+3e^{-\delta_k}+e^{-2\delta_k})(e^{\delta_k}-1)\Big\}. \tag{5.22}$$

Using (5.6) gives

$$e^{\delta_k}-1 = \cosh\delta_k+\sinh\delta_k-1 = \cosh\gamma_k-\frac{3}{2}+\sinh\delta_k.$$

Substituting the above equation into (5.21) and (5.22), and using the estimates (5.3) and (5.4), we obtain (5.18). □

Next we write $(\cosh\gamma_k+\cosh\delta_k)\mathcal{Q}_{m,k}$ as

$$(\cosh\gamma_k+\cosh\delta_k)\mathcal{Q}_{m,k} = \mathcal{Q}_{m,k}^0\exp[M(\gamma_k+\delta_k)]+\mathcal{Q}_{m,k}^1\exp[M(\gamma_k-\delta_k)]+\text{L.O.T.}$$

with

$$\begin{cases} \mathcal{Q}_{m,k}^0 = \dfrac{1}{4}(e^{\gamma_k}+e^{\delta_k})\left((-1)^m e^{-m\gamma_k}\mathcal{Q}_1 - e^{-m\delta_k}\mathcal{Q}_2\right), \\ \mathcal{Q}_1 = 3(1+e^{\delta_k})+e^{2\delta_k}-e^{-\delta_k}-6\rho_k(5+e^{\delta_k}), \\ \mathcal{Q}_2 = e^{2\gamma_k}+e^{-\gamma_k}-3(e^{\gamma_k}-1)+6\rho_k(e^{\gamma_k}-5), \end{cases}$$

and

$$\begin{cases} \mathcal{Q}^1_{m,k} = \dfrac{1}{4}(e^{\gamma_k} + e^{-\delta_k})\left(-(-1)^m e^{-m\gamma_k}\mathcal{Q}_3 - e^{m\delta_k}\mathcal{Q}_4\right), \\ \mathcal{Q}_3 = 3(1-2\rho)(e^{-\delta_k}-1) + e^{-2\delta_k} - e^{\delta_k} + 6(1-6\rho_k), \\ \mathcal{Q}_4 = -\mathcal{Q}_2. \end{cases}$$

We have the following estimate for $\mathcal{Q}^0_{m,k}$ and $\mathcal{Q}^1_{m,k}$.

Lemma 5.6. *There holds*

$$|\mathcal{Q}_1| + |\mathcal{Q}_2| + |\mathcal{Q}_3| + |\mathcal{Q}_4| \le C\left(\sqrt{\lambda_k} + \frac{1}{M-1}\right). \tag{5.23}$$

Proof. We only estimate $\mathcal{Q}_1$ and $\mathcal{Q}_2$. The terms $\mathcal{Q}_3$ and $\mathcal{Q}_4$ can be bounded similarly. Similar to (5.20), we have

$$\cosh[2\delta_k] = -\cosh\delta_k + \lambda_k + 2.$$

Using the above equation, we write $\mathcal{Q}_1$ as

$$\begin{aligned} \mathcal{Q}_1 &= 3(1+\cosh\delta_k + \sinh\delta_k) - \cosh\delta_k + \lambda_k + 2 + \sinh[2\delta_k] \\ &\quad - (\cosh\delta_k - \sinh\delta_k) - 6\rho_k(5 + e^{\delta_k}) \\ &= \lambda_k + 5 + \cosh\delta_k + 4\sinh\delta_k + \sinh[2\delta_k] - 6\rho_k(5+e^{\delta_k}) \\ &= \lambda_k + (5+e^{\delta_k})(1-6\rho_k) + \sinh\delta_k(3 + 2\cosh\delta_k). \end{aligned}$$

Using (5.20) and proceeding along the same line that leads to the above expression of $\mathcal{Q}_1$, we obtain

$$\begin{aligned} \mathcal{Q}_2 &= 2\cosh^2\gamma_k + 2 + \sinh[2\gamma_k] - 3(\cosh\gamma_k + \sinh\gamma_k) + \cosh\gamma_k - \sinh\gamma_k + 6\rho_k(e^{\gamma_k} - 5) \\ &= \lambda_k + 5 - \cosh\gamma_k + \sinh[2\gamma_k] - 4\sinh\gamma_k + 6\rho_k(e^{\gamma_k} - 5) \\ &= \lambda_k + (1-6\rho_k)(5 - e^{\gamma_k}) + 2\sinh\gamma_k(\cosh\gamma_k - 3/2). \end{aligned}$$

Using (5.3), (5.4) and (5.9), we get

$$|\mathcal{Q}_1| + |\mathcal{Q}_2| \le C\left(\sqrt{\lambda_k} + \frac{1}{M-1}\right).$$

This completes the proof of the lemma. □

To prove Theorem 5.1, we need the following identity that can be easily derived from [12, p. 38, formula 1.353(1)].

Lemma 5.7. *For any $\varrho \in (0,1)$, we have*

$$\begin{aligned} &\sum_{k=1}^{N} \varrho^{2k-1}\sin[(2k-1)x] \\ =&\frac{(\varrho+\varrho^3)\sin x - \varrho^{2N+1}\sin[(2N+1)x] + \varrho^{2N+3}\sin[(2N-1)x]}{1 - 2\varrho^2\cos[2x] + \varrho^4}. \end{aligned}$$

5.2. Proof of Theorem 5.1

Based on the above estimates, we are ready to prove Theorem 5.1. Using (5.11) and (5.18), we have, for $m \le -2$,

$$|Dy(m,n)| \le \frac{C}{N} \sum_{\substack{k=1 \\ k \text{ odd}}}^{2N-1} \exp(-|m|\alpha_k) \sin\frac{k\pi}{2N}. \tag{5.24}$$

By (5.11) and (5.23), we have, for $m \ge 0$,

$$|D_1 y(m,n)| \le \frac{C}{N} \sum_{\substack{k=1 \\ k \text{ odd}}}^{2N-1} \left(\exp(-m\gamma_k) + \exp(-m\delta_k) \sin\frac{k\pi}{2N} \right), \tag{5.25}$$

$$|D_2 y(m,n)| \le \frac{C}{N} \sum_{\substack{k=1 \\ k \text{ odd}}}^{2N-1} \left(\exp(-m\gamma_k) \sin\frac{k\pi}{2N} + \exp(-m\delta_k) \sin\frac{k\pi}{2N} \right). \tag{5.26}$$

Let $\varrho = \exp[-|m|/(2\sqrt{5}N)]$ and $x = \pi/[2N]$, and using Lemma 5.7, we have

$$\begin{aligned} &\sum_{\substack{k=1 \\ k \text{ odd}}}^{2N-1} \exp(-|m|\alpha_k) \sin\frac{k\pi}{2N} \le \sum_{k=1}^{N} \varrho^{2k-1} \sin[(2k-1)x] \\ =&\frac{\varrho(1+\varrho^2)(1+\varrho^{2N})}{(1-\varrho^2)^2 + 4\varrho^2 \sin^2 x} \sin x \le \frac{2\varrho(1+\varrho)^2}{(1-\varrho^2)^2} \sin x = \frac{2\varrho}{(1-\varrho)^2} \sin x. \end{aligned}$$

Using Lozarević's inequality [14]:

$$\cosh t \le \left(\frac{\sinh t}{t} \right)^3, \qquad t \ne 0,$$

and the elementary inequality $\cosh t \ge e^t/2, t \in \mathbb{R}$, we obtain

$$\begin{aligned} \frac{2\varrho}{(1-\varrho)^2} \sin x &= \frac{\sin\dfrac{\pi}{2N}}{2\sinh^2\left(\dfrac{|m|}{4\sqrt{5}N}\right)} \le \frac{\dfrac{\pi}{2N}}{\left(\dfrac{|m|}{4\sqrt{5}N}\right)^2 \cosh^{2/3}\left(\dfrac{|m|}{4\sqrt{5}N}\right)} \\ &\le \frac{2^{2/3} 40\pi N}{m^2} \exp\left[-\frac{|m|}{6\sqrt{5}N} \right] \le \frac{80\pi N}{m^2} \exp\left[-\frac{|m|}{6\sqrt{5}N} \right], \end{aligned}$$

which together with (5.24) leads to(5.1).

For $m \ge 1$ and let $\varrho = \exp[-m/(5N)]$, we immediately have (5.2).

The proof of the case when $m = -1$ can be done in the same way that leads to (5.1). We leave it to the interested readers. □

Proceeding along the same line that leads to Theorem 5.1, we have the following estimate on the solution.

Corollary 5.1. *There exists C such that*

$$\begin{aligned} &|y(m,n)| \le C\frac{\varepsilon}{|m|}, \quad m \le -1, \\ &|y(m,n)| \le C\varepsilon \left(\left(\frac{3-\sqrt{5}}{2} \right)^m + \frac{1}{m+1} \right), \quad m \ge 0. \end{aligned}$$

The above estimate suggests that the ghost force actually induces a negligible error on the solution, which is as small as ε.

Acknowledgments. The work of Ming was partially supported by National Natural Science Foundation of China grants 10932011 and 91230203, by the funds from Creative Research Groups of China through grant 11021101, and by the support of CAS National Center for Mathematics and Interdisciplinary Sciences. The authors are grateful to Weinan E and Jianfeng Lu for helpful discussions.

References

[1] M. Born and K. Huang, Dynamical Theory of Crystal Lattices, Oxford University Press, 1954.
[2] M. Dobson and M. Luskin, An analysis of the effect of ghost force oscillation on quasicontinuum error, *ESAIM: M2AN*, **43** (2009), 591–604.
[3] W. E, Principles of Multiscale Modeling, Cambridge University Press, 2011.
[4] W. E, J. Lu and J.Z. Yang, Uniform accuracy of the quasicontinuum method, *Phys. Rev. B*, **74** (2006), 214115.
[5] W. E and P.B. Ming, Analysis of multiscale methods, *J. Comput. Math.*, **22** (2004), 210–219.
[6] W. E and P.B. Ming, Analysis of the local quasicontinuum methods, in *Frontiers and Prospects of Contemporary Applied Mathematics*, Higher Education Press, World Scientific, Singapore, Tatsien Li and P.W. Zhang eds., 2005, 18–32.
[7] W. E and P.B. Ming, Cauchy-Born rule and the stability of crystalline solids: static problems, *Arch. Ration. Mech. Anal.*, **183** (2007), 241–297.
[8] J.L. Ericksen, On the Cauchy-Born rule, *Math. Mech. Solids*, **13** (2008), 199–220.
[9] J.L. Ericksen, The Cauchy and Born hypotheses for crystals, in *Phase Transformations and Material Instabilities in Solids*, Academic Press, M.E. Gurtin eds., Ohio, 1984, 61–77.
[10] G. Friesecke and F. Theil, Validity and Failure of the Cauchy-Born hypothesis in a two-dimsnsional mass-spring lattice, *J. Nonlinear Sci.*, **12** (2002), 445–478.
[11] B.I. Henry and M.T. Batchelor, Random walks on finite lattice tubes, *Phy. Rev. E*, **68** (2003), 016112.
[12] A. Jeffrey and D. Zwillinger, Table of Integrals, Series, and Products, 7th eds., Elsevier (Singapore) Pte Ltd., 2007.
[13] J. Knap and M. Ortiz, An analysis of the quasicontinuum method, *J. Mech. Phys. Solids*, **49** (2001), 1899–1923.
[14] I. Lazarević, Neke nejednakosti sa hiperbolickim funkcijama, *Univerzitet u Beogradu. Publikacije Elektrotehničkog Fakulteta. Serija Matematika i Fizika*, **170** (1966), 41–48.
[15] J.E. Lennard-Jones, On the determination of molecular fields-II. from the equation of state of a gas, *Proc. Roy. Soc. London Ser. A*, **106** (1924), 463–477.
[16] J. Lu and P.B. Ming, Convergence of a force-based hybrid method for atomistic and continuum models in three dimension, preprint, arXiv:1102.2523, to appear in *Comm. Pure Appl. Math.*.
[17] W.H. McCrea, and F.J.W. Whipple, Random paths in two and three dimensions, *Proc. Roy. Soc. Edingburgh*, **60** (1940), 281–298.
[18] R.E. Miller and E.B. Tadmor, A unified framework and performance benchmark of fourteen multiscale atomistic/continuum coupling methods, *Modelling Simul. Mater. Sci. Eng.*, **17** (2009), 053001–053051.
[19] P.B. Ming, Error estimate of force-based quasicontinuum method, *Commun. Math. Sci.*, **6** (2008), 1087–1095.
[20] P.B. Ming and J.Z. Yang, Analysis of a one-dimensional nonlocal quasicontinuum method, *Multiscale Model. Simul.*, **7** (2009), 1838–1875.

[21] A.V. Shapeev, Consistent energy-based atomistic/continuum coupling for two-body potentials in one and two dimensions, *Multiscale Model. Simul.*, **9** (2011), 905–932.

[22] V.B. Shenoy, R. Miller, E.B. Tadmor, D. Rodney, R. Phillips, and M. Ortiz, An adaptive finite element approach to atomic-scale mechanics – the quasicontinuum method, *J. Mech. Phys. Solids*, **47** (1999), 611–642.

[23] T. Shimokawa, J.J. Mortensen, J. Schiøz and K.W. Jacobsen, Matching conditions in the quasicontinuum method: Removal of the error introduced at the interface between the coarse-grained and fully atomistic region, *Phys. Rev. B*, **69** (2004), 214104.

[24] E.B. Tadmor, M. Ortiz, and R. Phillips, Quasicontinuum analysis of defects in solids, *Philos. Mag. A*, **73** (1996), 1529–1563.